Inter-correlation of hydrothermal mineral alteration zone in the vicinity of lineaments

Mahesh Kumar Tripathi* and H. Govil

Department of Applied Geology, National Institute of Technology, Raipur 492 010, India

There are significant and effective roles of geological structures such as lineaments in mineral zone identification and interpretation, exploration and mapping of rock units, litho-boundaries, local tectonic zones and fractures, and hydrothermal alteration facies. The aim of this study was to extract lineaments of Jahajpur region of Bhilwara district, Rajashtan automatically and digitally using Sentinel 2A optical data. The automatic lineament extraction by 'LINE' algorithms tool with involvement of several processing steps and parameters of PCI Geomatica evaluated digitally extracted lineaments, geospatial analyses such as length of lineaments, lineament density and lineament orientation. The obtained results were validated through assessment of geomorphic and structural features interpretation by numerical, analogical, and geospatial analysis and field survey for a better understanding and correlation. The vicinity of extracted lineament and lineament densities show the various alteration minerals such as clay, talc, mica, dolomite and goethite. Thus, we can conclude that lineaments have excellent inter-relationship with hydrothermal alteration and weathering zones in the western Jahajpur belt, Rajasthan.

Keywords: Geospatial analysis, hydrothermal alteration, lineaments, optical data, weathering zones.

THERE are several studies on lineaments for geological, hydrological, geotechnical and environmental research[1]. Geology is the key component factor to map the lineaments or other related geomorphic features[2]. In the beginning, geologists studied the linear features which are penetrative and pervasive within the earth's surface. According to Hung *et al.*[3], alignment of lineaments is straight or curvilinear and that lineament can be the line of faults, fractures and weakness of ridge line. Ridges, cliffs, terraces and aligned segments of valleys are implications of geomorphological features of lineaments[3]. The linear pattern of vegetation and vegetation differences, moisture content, tonal and contrast variation in soils and rocks define the signature of lineaments for interpretation[4–8]. According to Neawsuparp and Charusiri[9], there are several applications of lineament extractions, such as in geological structures, tectonics, hydrothermal alteration minerals, lithological boundaries and groundwater potential zone mapping[10,11]. Lineament analysis is the measurement of the zone of ore mineralization, and permeability of rocks can be identified through orientation of strike length of lineaments, length of lineaments and lineament density[11].

The importance of higher spectral and spatial resolution of remote sensing data has been proven in various geological applications such as lineament extraction, geological exploitation and mineral mapping[2]. There is significant application of higher spatial and narrow spectral resolution such as optical infrared for lineament extraction[2]. The shortwave infrared bands (1.0–2.5 μm) are more valuable for lineament extraction[2]. The Sentinel 2A optical infrared data have significant capabilities inspectral/spatial (optical infrared band 2 – 0.458–0.523 μm/10 m, band 3 – 0.543–0.578 μm/10 m and band 4 – 0.650–0.680 μm/10 m) resolution. The extraction of lineaments can be done using remote sensing techniques such as analogical and geospatial analyses. In analogical analysis, the remote sensing data can acquire information on a regional basis and is therefore a better tool to delineate lineaments through image and geotechnical elements. These elements are important in the identification and interpretation of geological features because understanding two-dimensional images is difficult. The image elements such as tone, texture, shape, size, shadow pattern and association help in the visualization of targets. The geotechnical elements such as ridge, valley, drainage pattern, beddings, slops (flat iron), litho boundaries, folds, faults, fractures and joints have inter-relationship with geologic features such as ridge and valley river channel, drainage pattern, etc.

Delineation of lineaments is better using satellite images compared to aerial photographs[12]. According to Kruse[13] 'the use of enhanced images, hybrid classifiers, integration of GIS and remote sensing data, and use of narrower spectral band width data has aided geological mapping, an application where the mineralogy, weathering characteristics and geochemical signatures are useful in determining the nature of rock units'[13].

Researchers have used satellite data to provide information on various parameters such as resolution, bands, colour combination, digital image processing techniques such as LINE algorithms tool of PCI Geomatica, spatial filtering, normalize vegetation index (NDVI), band ratio, false colour composite (FCC), principal component analysis

*For correspondence. (e-mail: tripathi.mahesh1@gmail.com)

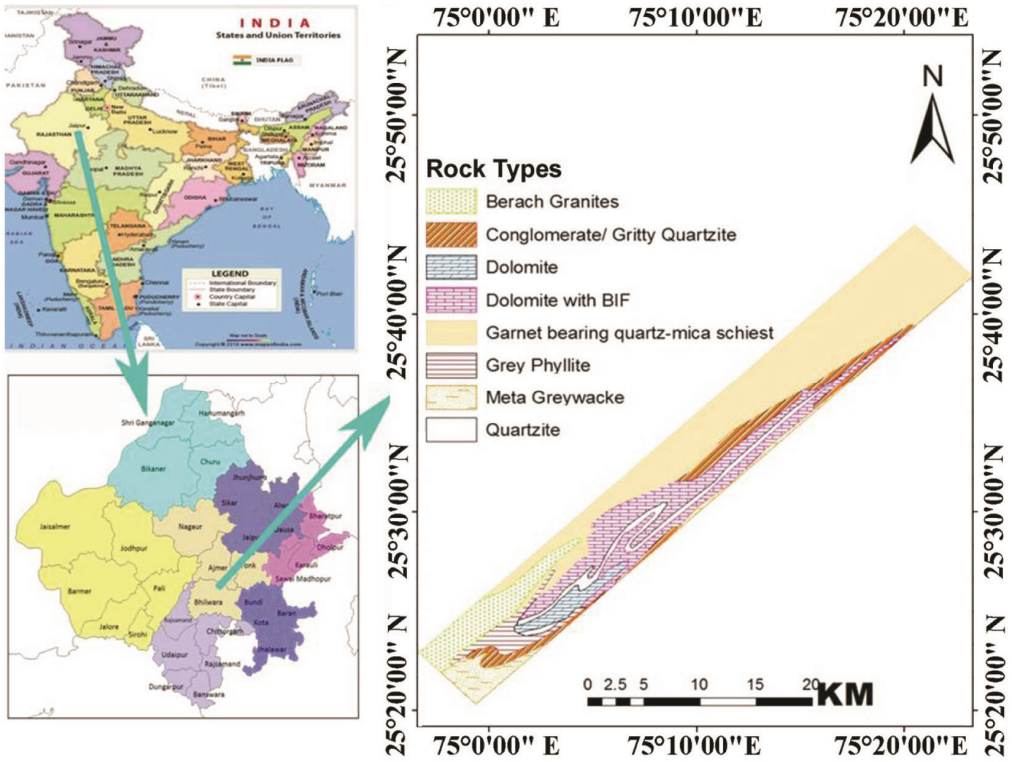

Figure 1. Geological map of the study area[52,53].

(PCA) and minimum noise fraction (MNF) for the extraction of geomorphic/geologic features[1,2,5,6,14–17]. Each band has specific characteristics to highlight and enhance the information.

The present study aims to establish the inter-relation of hydrothermal alteration zone in the vicinity of lineaments. Several researchers have identified, hydrothermal alteration mineral zones in the western Jahajpur belt region of Bhilwara, Rajasthan, India[18–21]. The hydrothermal alteration mineral mapping helped identify clay group of minerals such as montmorillonite, kaosmec, dolomite, talc and goethite[18]. According to Robb[22], silica precipitants belonging to quartz veins are formed in the presence of hot aqueous solution percolating through fractures. An increment of pressure and temperature converts water into a powerful solvent which dissolves significant amounts of rock-forming minerals other than silica, such as alkali metals[22].

The objective of this study is to delineate or extract lineaments and establish correlations among the various hydrothermal mineral alteration zones. It also focuses on the identification of alteration and weathered zone in the study area.

Geological setting

The present study was performed in Jahajpur (25.62°N, 75.28°E) at an average elevation of 334 m (1095 ft) (Figure 1).

The geological settings of Jahajpur region belong to Precambrian rock sequences, Mangalwar complex, Hindoli group, Jahajpur group and Vindhyan supergroup[18,19,23,24]. The folded occurrence of quartzite, dolomite and banded iron formation (BIF) of Jahajpur sequence on conformity over Hindoli groups[25,26]. There exist crenulations, cleavage and regional schistosity and folds of four generations. Also, there are two parallel ridges of dolomitic limestone and quartzite striking in the northeast direction along and across River Banas[27–32].

Data and methodology

The European Space Agency (ESA) launched the Sentinel-2 mission under the Copernicus programme for observation of the Earth to monitor and map forests, land-cover change detection and management of natural disasters. It has two satellites, viz. Sentinel-2A and Sentinel-2B. The multi-spectral instrument (MSI) sensors provide geometrically and radiometrically corrected Sentinel 2A images with high spatial resolution (10, 20 and 60 m) with 13 bands in the optical NIR (near-infrared) and SWIR (shortwave infrared) of the EMR (electromagnetic region) and with wide coverage of about 290 km (ref. 33). Three optical infrared bands 2, 3 and 4 are used in this study for automatic lineament extraction.

In the adopted methodology, initially image processing involves radiometric correction operations to reduce the

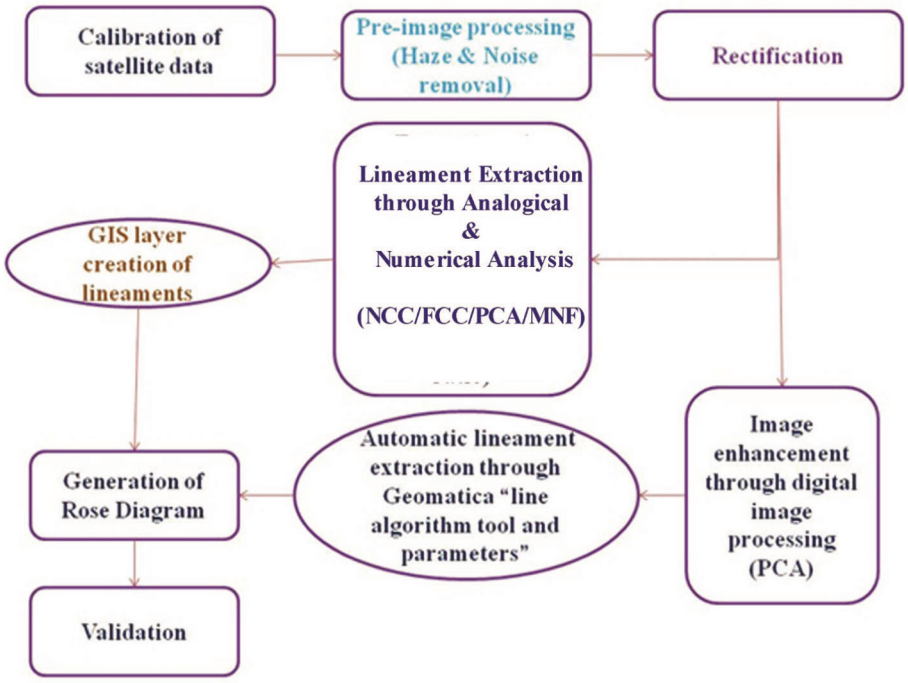

Figure 2. Flow diagram of the methodology.

Table 1. Specification of sentinel 2A sensors

Sensor	Band	Spectral range (μm)	Spatial resolution (m)
Coastal aerosol	1	0.443	60
Blue	2	0.490	10
Green	3	0.560	
Red	4	0.665	
Vegetation red edge	5	0.705	20
Vegetation red edge	6	0.740	
Vegetation red edge	7	0.783	
Near-infrared (NIR)	8	0.842	10
Vegetation red edge	8A	0.865	20
Water vapour	9	0.945	60
Shortwave infrared (SWIR)-cirrus	10	1.375	
SWIR	11	1.610	20
SWIR	12	2.190	

errors caused by atmospheric disturbances. In the next steps, several image-enhancement techniques (noise, haze correction) are applied to increase the visibility of the image element. To increase the visibility and disturbance of geotechnical features, various enhancement techniques (PCA, band combination and MNF) were evaluated for better observation (Figure 2)[1].

For lineament enhancement and extraction, PCA was performed on optical infrared bands of Sentinel data in PCI Geomatica software (Table 1). In the next step, image-processing methods to edge enhancement, detection and direction of lineaments were implemented. The third step involves line module parameters for lineament extraction. The fourth step includes calculation of length, density and direction of lineaments[2,5,8,11,34,35].

Procedure for automatic lineament extraction

Analogical analyses were done for edge detection and image enhancement, while PCA, FCC and MNF were used for visual interpretation. The length and number of lineaments in the study area depend upon the adopted parameters of LINE algorithm module of PCI Geomatica. The values of input parameters of LINE algorithm of PCI Geomatica define the length and number of extracted lineaments. The values of input parameters are optional (which can be used according to environmental conditions such as arid climate, humid). The LINE algorithm involves three stages of lineament extraction: (i) edge detection, (ii) thresholding and (iii) curve extension. Using the optional six parameters which are mentioned below

Table 2. Optional input parameters in PCI-Geomatica LINE tool

Parameters (pixel)	Values	Ranging values
RADI-filter radius	10	0–100
GTHR-edge gradient threshold	100	0–255
LTHR-curve length threshold	30	0–100
FTHR-line fitting error threshold	3	1–100
ATHR-angular difference threshold (degree)	30	0–90
DTHR-linking distance threshold	20	0–100

the LINE algorithm, we can convert the extracted linear feature into vector form[6]. These applied parameters are RADI (filter radius), GTHR (gradient threshold), LTHR (length threshold), FTHR (line fitting error threshold), ATHR (angular difference threshold) and DTHR (linking distance threshold). RADI parameters and/or used to specify the edge detection filter radius (pixel). GTHR parameter specifies minimum gradient threshold to obtain a binary image through an edge pixel. LTHR defines the minimum length of a curve (in pixels) for consideration of lineament. FTHR is applied for fitting of pixel curve through a polyline. ATHR parameter have specification to generate the maximum angle (degree) between polyline. DTHR parameters are applied to generate the minimum distance (in pixels) between end points of two vectors where two vectors are linking to each other. The extracted lineaments are saved as shape file in Arc GIS software for further geospatial analysis and data processing[3,6,35]. Table 2 shows the applied threshold values of LINE tool parameters.

Results and discussion

Various researchers applied automatic lineament extraction for observation of lineaments and associated geological structures and litho-boundaries identification[3,35,37]. According to different environmental and climatic conditions, the parameters of the optional threshold values are applied for automatic lineament extraction in PCI Geomatica. The automatic lineament extraction increases the quality and quantity of lineaments in wide range or zonal basis measurement compared to conventional geological lineament extraction methods. In this scenario, spatial capability of satellite image resolution plays an important role for extraction of lineaments. Researchers have used different optional values for parameters for automatic lineament extraction[3,35–37].

Extraction of lineaments

For manual interpretation, remote sensing data and techniques play a significant role in the enhancement of geomorphic and anthropogenic features because manual interpretation involves 'to scan large area quickly and recognize discontinuous linear pattern such as truncations and offsets'[16]. Interpretation of geomorphic features such as enhancement or manual extraction of lineaments requires band combination, FCC, MNF, etc.

Analogical analysis

True colour composite: The analogical analysis method applied for extraction, assessment, detection and enhancement of lineaments which can be observed through image elements and photo elements such as shape, size, colour, tone, texture, contrast, pattern and association of lineaments or geological structures. The natural colour composite image shows variation in tonal contrast to interpret the ridge and valley structures (Figures 3 and 4).

False colour composite: FCC enhances variation in the visibility of geomorphic features for interpretation with mutual application of image and geotechnical elements. The quality of geomorphic features depends on the resolution of remote sensing data. Researchers have used FCC band combinations[2,11,15,38]. This geomorphic feature can be extracted using remote sensing and GIS software[1]. The FCC image only highlights major ridges in the study area along the river channel, which can be differentiated by variation in tonal contrast.

Principal component analysis: PCA technique is used to reduce the redundancy and dimensionality of remote sensing data. It has the capability to enhance contrast and reduce data without loss of information. Several researchers have used the PCA technique to enhance images for geomorphic feature interpretation[2,11,15,17,37–42]. The PCA techniques help enhance major geomorphic structures such as ridge, truncation in river channel, fault and U-shaped structures near Jahajpur to Ampura, Jamoli, Ampura, Meera Nagar, Kanti and Itwa in the study area. The ridge structure and U-shaped features show maximum contrast as brownish-red colour and the width of ridge is narrowing at the adjacent places with respect to the surroundings. The river channel is also interpreted as dull violet colour. At Chohli, the river is directed from west to east and there is variation in direction of river flow channel within few kilometers such as north to south and south to north. Some linear alignments are indicating the litho-boundaries in study area which are represented as magenta

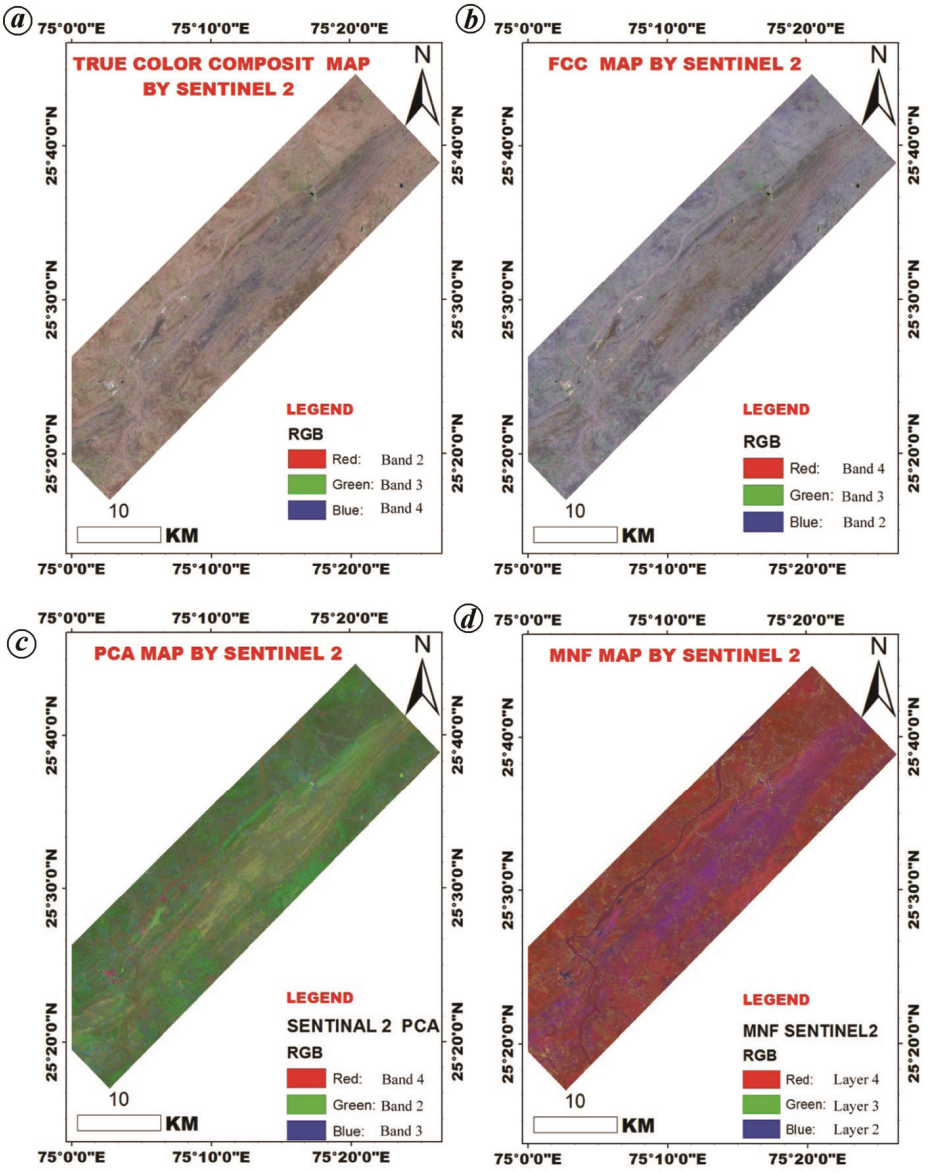

Figure 3. Enhancement of lineaments by (***a***) true colour composite map, (***b***) false colour composite map, (***c***) principal component analysis (PCA) map and (***d***) minimum noise fraction image of Sentinel 2A image.

colour. Some place linear alignment as magenta colour which is an indication of litho-boundaries in the study area. The mining area is highlighted in cyan in the region.

The minor fractures and drainages are prominent as yellowish-green in colour. The U-shaped features are highlighted in brownish-red and mining zones of Chainpura, Ampura and Madhopura in pink colour with linear alignment.

Minimum noise fraction: The MNF has shown capability to interpret the litho-boundaries at several places along the major ridge with slight variation in light blue and cyan colour. The other litho-boundaries are also interpreted as a variation in maximum tonal contrast as pink colour. The mining areas are interpreted as brownish-red. The river channel is highlighted in violet colour.

Geospatial analysis

Length of lineaments: The total number of extracted lineaments in the study area divided by the total study area is denoted as the length of the lineaments. The length of a lineament is a significant characteristic of lineament interpretation. The lengths of lineaments in particular bands are different (Figures 5 and 6). A maximum length of 8347.94 m and 335 lineaments were observed in Sentinel 2A band 2.

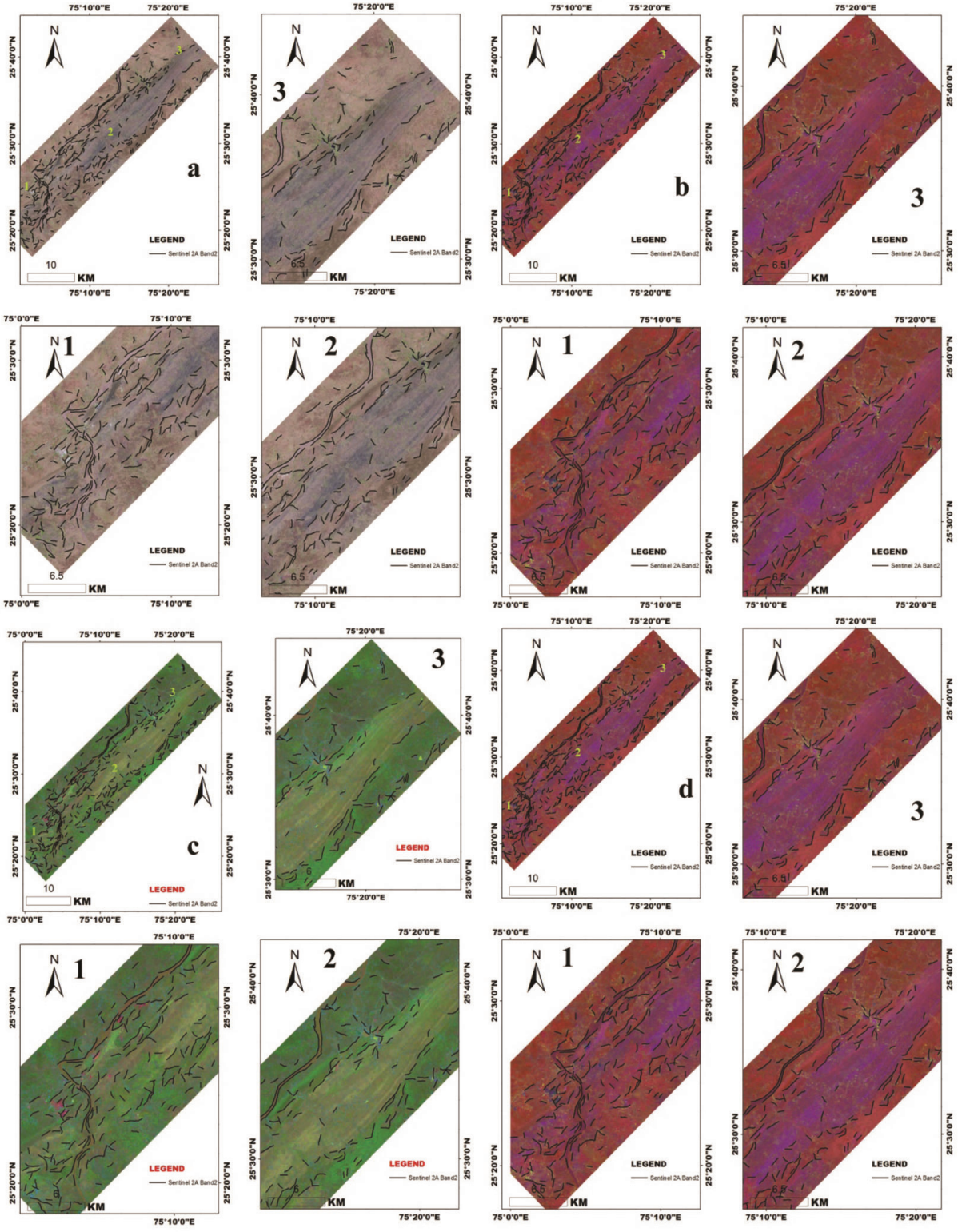

Figure 4. Overlapping of automatic extracted lineaments, highlighted lineament structures and features by analogical and numerical analysis of Sentinel 2A images.

Lineament density analysis: Lineament density is the most accepted parameter for measurement and distribution of lineaments per unit area[3,43,44]. The lineament frequency of per unit area defined by lineament density. The highest lineament density is observed in images where some geomorphic features are present (Figure 7).

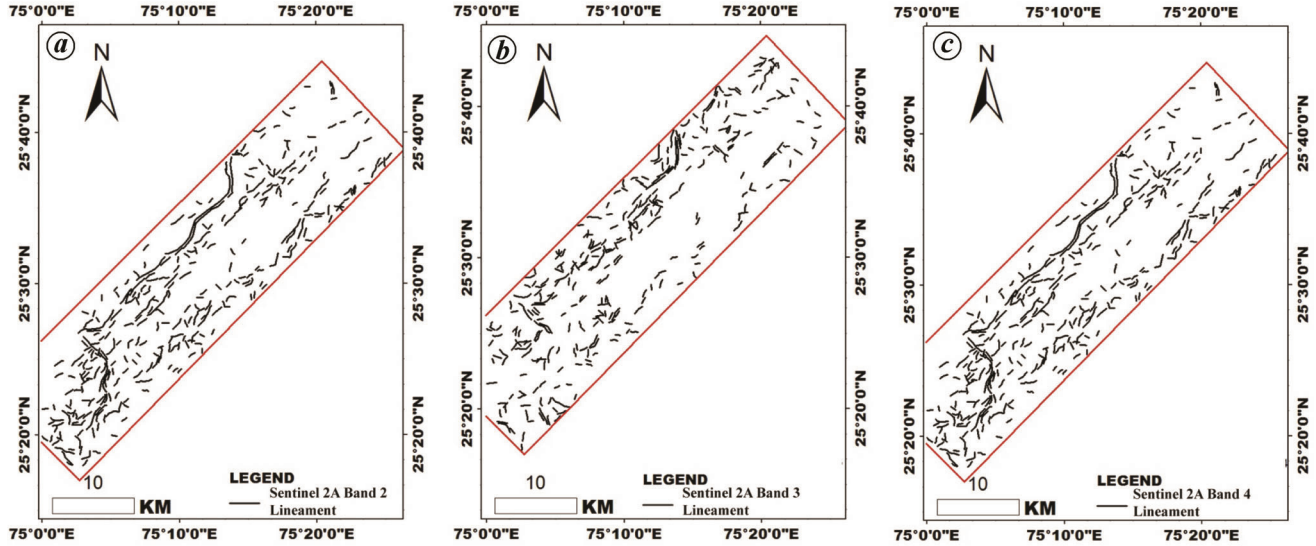

Figure 5. Automatic extracted lineament map of Sentinel 2A bands 2, 3 and 4.

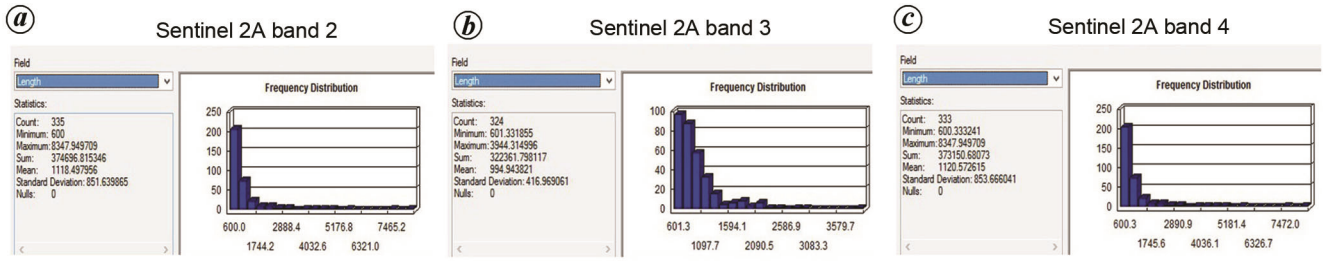

Figure 6. Length analysis of lineaments.

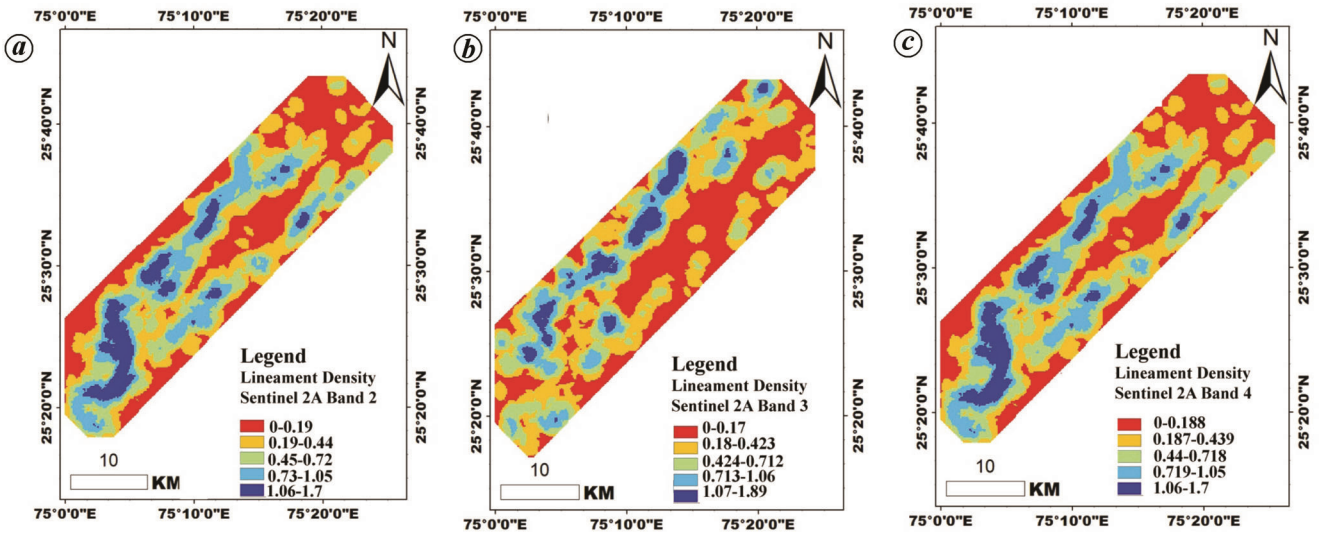

Figure 7. Lineament density map of Sentinel 2A: (*a*) band 2, (*b*) band 3 and (*c*) band 4.

Orientation analysis of lineament extraction: The frequency and orientation of strike length of the lineaments were observed using rose diagram. Most of the lineaments are trending in the NE–SW direction. The azimuthal trend of lineaments in each band of Sentinel 2A is mostly the same. Majority of the lineaments are striking in the NE–SW direction and density is also maximum where length of lineaments and frequency are higher (Figure 8).

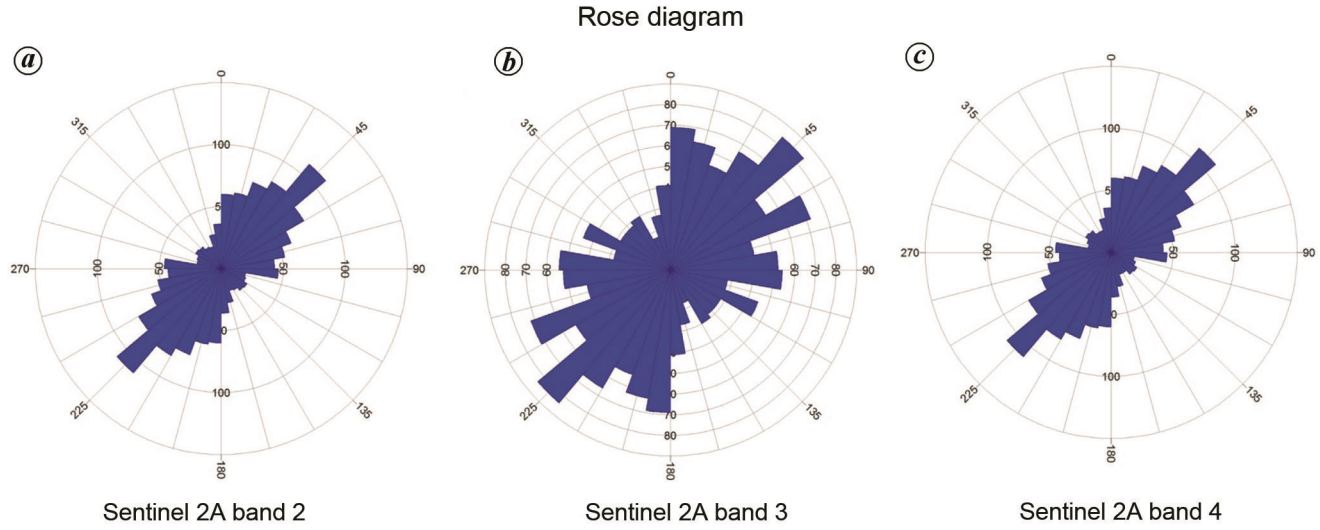

Figure 8. Orientation of strike length of Sentinel 2A bands 2, 3 and 4.

Validation

The various geomorphic features such as ridges are identified and validated, which are interpreted and digitally extracted using remote sensing data and techniques.

Genesis and formation of mineral alteration through hydrothermal process

The identification of minerals is based on the characteristics of mineral deposits, formation processes and formation environments such as hydrothermal systems. On the basis of characteristics of mineral zones, there are some mineral deposit models such as hydrothermal system (alteration zone), copper veins, replacement deposits and magmatic deposits. Each model is related to a specific zone of formation and process which helps in the prediction of significant ore distribution on the scale of deposits[45]. The hydrothermal alteration processes and minerals occur mostly in the vicinity of linear features such as lineaments, thrusts, faults and shear zones which are also called wall-rock alteration. The process of wall-rock alteration occurs through circulation of hot aqueous fluids which have significance in removal, addition and redistribution of components in rock alteration due to variation and change in chemistry, mineralogy and texture[22]. The variation changes (multiple changes with respect to time) in physics and chemistry of rocks or minerals indicate the occurrences of specific deposits (hydrothermally altered and weathered minerals) over a period of time. The hydrothermal fluids play a significant role in mineral stability through pressure, temperature and chemistry which affect the disintegration of rocks on or beneath the earth's surface, such as chemical weathering[22]. According to Rakovan[46], the hydrothermal process (metasomatism) occurs due to increments in temperature, pressure in presence of water causes the changes in chemistry of surface or subsurface surrounding rocks by lineaments, fractures and structural deformation. There are some case studies on lineaments related to hydrothermal alterations such as skarn deposits, lead and zinc deposits, and clay deposits[18,19,23,46–51]. Several studies have identified alteration minerals (kaolinite–smectite, montmorillonite, talc) and alteration facies (advanced argillic, propylitic by geochemical analysis (X-diffraction (XRD), X-ray flouroscane (XRF) and induced couple plasma mass spectroscopy). The advanced airborne visible infrared spectroscopy-new generation (AVIRIS-NG) hyper spectral image applied for regolith and hydrothermally altered, weathered and clay mineral mapping and identification with analysis of geochemistry of western Jahajpur belt of Bhilwara, Rajashtan[18,19,23,46–51].

Hydrothermal alteration zones

There is a broader significance of lineament or geomorphic and geological structural features in the study of hydrothermal alteration zones. The occurrence and formation of hydrothermal alteration zones is associated with linear features. Some researchers identified and mapped hydrothermal alteration zones and alteration minerals such as kaosmec, montmorillonite, dolomite, talc and goethite with validation and verification of field photographs and by conventional techniques such as XRF, XRD, spectroscopy and ICPMS analysis[18,19,23,27,46–51]. The location of these identified hydrothermal alteration minerals was plotted with extracted lineaments in the GIS platform using Sentinel 2A images. All hydrothermal alteration mineral locations in the study area are situated at or in the vicinity of lineaments (Figure 9 and Table 3). The extracted zone of lineaments is associated with clay minerals of

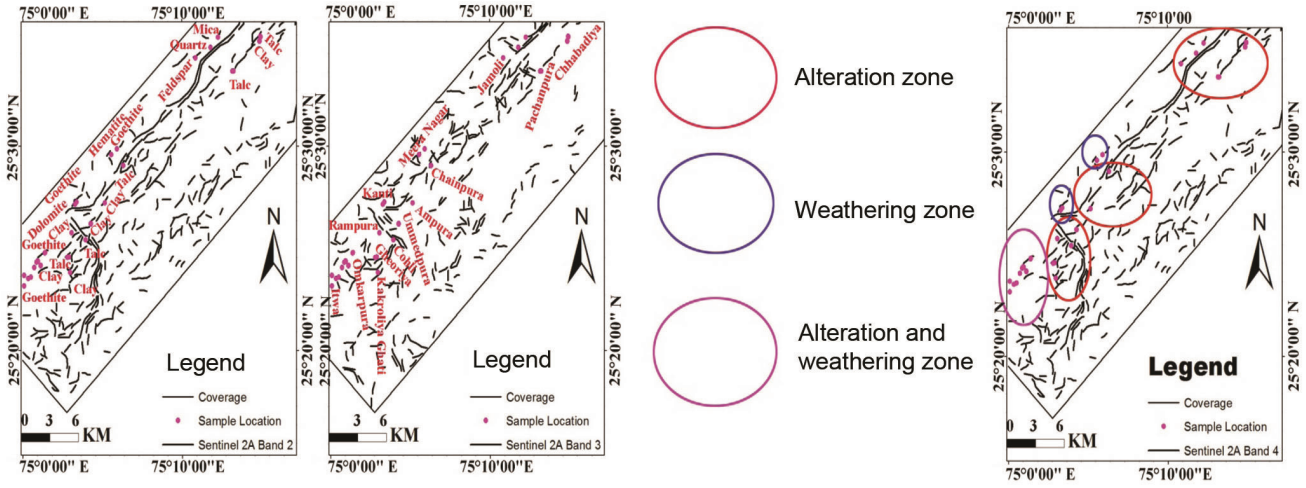

Figure 9. Mineral sample locations in the vicinity of lineament features of the study area, western Jahajpur belt.

Table 3. Sample location of alteration minerals

Location	Mineral	Location	Mineral
Chhabadiya	Talc	Jamoli	Feldspar
Chhabadiya	Talc	Meera Nagar	Hematite
Chhabadiya	Clay	Meera Nagar	Goethite
Chhabadiya	Clay	Kanti	Dolomite
Chhabadiya	Clay	Kanti	Goethite
Pachanpura	Talc	Ampura	Clay
Pachanpura	Talc	Cohli	Talc
Pachanpura	Talc	Ummedpura	Clay
Gheoriya	Talc	Omkarpura	Goethite
Gheoriya	Talc	Itwa	Goethite
Omkarpura	Clay	Jamoli	Quartz
Omkarpura	Clay	Bonai Kheda	Goethite
Omkarpura	Clay	Omkarpura	Goethite
Omkarpura	Goethite	Itwa	Goethite
Omkarpura	Clay	Itwa	Clay
Omkarpura	Clay	Itwa	Goethite
Omkarpura	Clay	Kakrpoliya Ghati	Clay
Rampura	Clay	Chainpura	Talc
Itwa	Clay	Jamoli	Mica

Ampura, Ummedpura, Chhabadiya, Rampura, Itwa and Omkarpura; talc minerals of Chhabadiya, Pachanpura, Chainpura, Ummedpura, Chohli and Gheoriya; goethite minerals in Kanti, Meera Nagar, Bonai Kheda, Omkarpura and Itwa, and Dolomite minerals in Kanti region (Figure 10). Studies have discriminated the alteration and weathered zones near Omkarpura, Itwa and Kanti by geochemical interpretation using ICPMS, XRF and XRD analysis[18,49].

Conclusion

Geospatial analyses, automatic lineament extraction method and analogical analysis play a significant role in remote sensing technology. To extract lineaments at unreachable and lunar surfaces, lineaments and structures can be identified and interpreted using remote sensing images. Remote sensing images also have better capability to extract information on the basis of specification and sensitivity of particular bands of the EM spectrum according to spatial and spectral resolution. The minute and unpredictable or subtle features cannot be identified through the original remote sensing image. It requires digital image processing to remove redundancy and enhancement of image for further applications. In the process of automatic lineament extraction, PCA plays an important role to remove redundancy of data and edge enhancement and detection in the image, which shows better response in the results. MNF, FCC and RGB colour combination have also shown better results to identify the linear features and litho-boundaries using Sentinel 2A data.

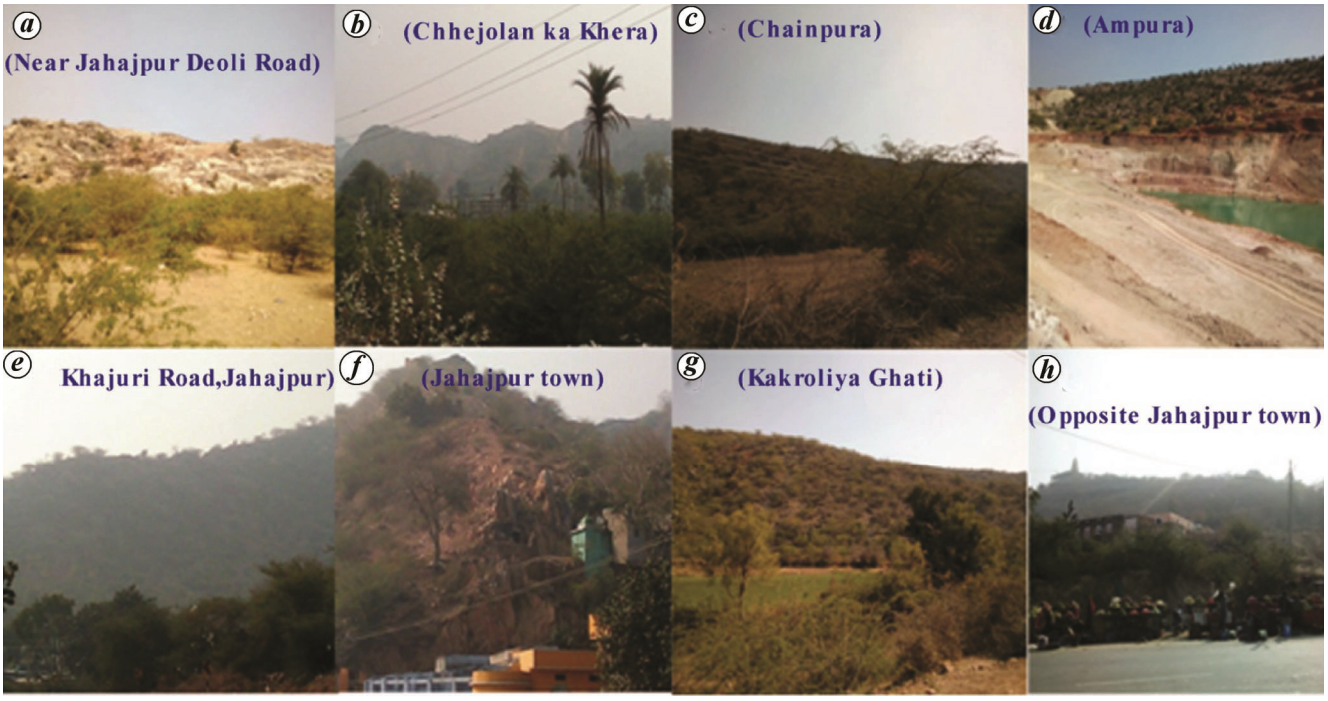

Figure 10. Ridge geomorphic structures at Jahajpur region: (***a***) Deoli road, (***b***) Chhejolan ka Khera, (***c***) Chainpura, (***d***) Ampura, (***e***) Khajuri Road, (***f***) Jahajpur town, (***g***) Kakroliya Ghati and (***h***) Jahajpur.

The strike length of the lineaments and flow of the river at some places are parallel in the study area. This shows a linear combination of geomorphic features. So, this result proves that a higher-resolution image can play an important role to identify and extract subsurface lineaments which are in beneath the earth's surface. Sentinel 2A data have shown better results in automatic lineament extraction in optical NIR bands 2, 3 and 4. The extracted lineaments have shown potential in validation and hydrothermal alteration zone formation inter-relation in lineament vicinity among availability of suitable optical infrared bands and their selection. The hydrothermal alteration minerals zone and weathered minerals zone of the study area have shown significant correlation with extracted lineaments vicinity and density. The higher-resolution remote sensing data in combination with the narrow optical infrared and SWIR region of the EM spectrum have the potential to extract the subsurface and buried linear or curvilinear features such lineaments, litho-boundaries, ridges, etc. The density of the lineament has the potential to determine the alteration zone, groundwater potential zone and weathering zone of economically profitable minerals. Mutual studies of lineaments and lithology using remote sensing data have the ability to solve more critical problems in geology.

1. Baghdad, B., Structural interpretation of lineaments by remote sensing and GIS using Landsat 8 data: a case study of akreuch area (Morocco). *Eur. J. Sci. Res*., 2016, **138**(3), 216–224.
2. Mwaniki, M. W., Moeller, M. S. and Schellmann, G., A comparison of Landsat 8 (OLI) and Landsat 7 (ETM+) in mapping geology and visualising lineaments: a case study of central region Kenya. *Int. Arch. Photogramm., Remote Sensing Spat. Inf. Sci. – ISPRS Arch*., 2015, **40**(7W3), 897–903; doi:10.5194/isprsarchives-XL-7-W3-897-2015.
3. Hung, L. Q., Batelaan, O. and de Smedt, F., Lineament extraction and analysis, comparison of LANDSAT ETM and ASTER imagery. Case study: Suoimuoi tropical karst catchment, Vietnam. In Proc. SPIE 5983, Remote Sensing for Environmental Monitoring, GIS Applications, and Geology V, 59830T, 2005; https://doi.org/10.1117/12.627699.
4. O'Leary, D. W., Friedman, J. D. and Pohn, H. A., Lineament, linear, lineation: some proposed new standards for old terms. *Geol. Soc. Am. Bull.*, 1976, **87**, 1463–1469.
5. Thannoun, R. G., Automatic extraction and geospatial analysis of lineaments and their tectonic significance in some areas of northern Iraq using remote sensing techniques and GIS. *Int. J. Enhance. Res. Sci. Technol. Eng.*, 2013, **2**(2), 1–11.
6. Ibrahim, M., El-Bastawesy, M. A. and El-Saud, W. A., Automated, manual lineaments extraction and geospatial analysis for Cairo–Suez district (northeastern Cairo–Egypt), using remote sensing and GIS. *Int. J. Innov. Sci. Eng. Technol*., 2016, **3**(5), 491–500.
7. Hashim, A. M. S., Johari, M. A. M. and Pour, A., Automatic lineament extraction in a heavily vegetated region using landsat enhanced thematic mapper (ETM+) imagery. *Adv. Space Res.*, 2013, **51**, 874–890.
8. Abarca, M. A. A., Lineament extraction from digital terrain models. Case study, Lineament Extraction from Digital Terrain Models, San Antonio del Sur area, south-eastern Cuba, 2006.
9. Neawsuparp, K. and Charusiri, P., Lineaments analysis determined from Landsat data implication for tectonic features and mineral occurrences in Northern Loei Area, NE Thailand. *Sci. Asia*, 2004, **30**, 269–278.
10. Masoud, A. A. and Koike, K., Auto-detection and integration of tectonically significant lineaments from SRTM DEM and remotely-sensed geophysical data. *ISPRS J. Photogramm. Remote Sensing*, 2011, **66**, 818–832.

11. Alshayef, M. S., Mohammed, A. M., Javed, A. and Albaroot, M. A., Manual and automatic extraction of lineaments from multispectral image in part of Al-Rawdah, Shabwah, Yemen by using remote sensing and GIS technology. *Comput. Geosci*., 2017, **2**, 67–73.
12. Casas, A. M., Cortes, A. L., Maestro, A., Soriano, M. A., Riaguas, A. and Bernal, J., A program for lineament length and density analysis. *Comput. Geosci*., 2000, **26**(9/10), 1011–1022.
13. Kruse, F. A., Advances in hyperspectral remote sensing for geologic mapping and exploration. What is imaging spectrometry (hyperspectral sensing)? Atmospheric corrections are required for most hyperspectral analyses. In 9th Australasian Remote Sensing Conference, Sydney, Australia, 1998, vol. 1; http://www.hgimaging.com/PDF/Kruse_9th_australasian_rs_98.pdf
14. Corgne, S., Magagi, R., Yergeau, M. and Sylla, D., An integrated approach to hydro-geological lineament mapping of a semi-arid region of West Africa using Radarsat-1 and GIS. *Remote Sensing Environ*., 2010, **114**(9), 1863–1875; doi:10.1016/j.rse.2010.03.004.
15. Ramasamy, S. M., Bakliwal, P. C. and Rao, K. L. V. R., Use of remote sensing tectonic evolution and resources study of a part of Vindhychal basin, Jhalawar area, India. *J. Indian Soc. Remote Sensing*, 1988, **16**(1), 63–71.
16. Middleton, M., Schnur, T. and Sorjonen-Ward, P., Geological lineaments interpretation using the object-based image analysis approach: results of semi-automated analysis versus visual interpretation. *Geol. Surv. Finland*, *Spec. Paper*, 2015, **67**, 135–154.
17. Mavrantza, O. and Argialas, D., An object-oriented image analysis approach for the identification of geologic lineaments in a sedimentary geotectonic environment. In *Object-Based Image Analysis* (eds Blaschke, T., Lang, S. and Hay, G. J.), Lecture Notes in Geoinformation and Cartography, Springer, Berlin, Heidelbarg, 2008; https://doi.org/10.1007/978-3-540-77058-9_21.
18. Tripathi, M. K., Govil, H. and Chattoraj, S. L., Identification of hydrothermal altered/weathered and clay minerals through airborne AVIRIS-NG hyperspectral data in Jahajpur, India. *Heliyon*, 2020, **6**, e03487; doi:10.1016/j.heliyon.2020.e03487.
19. Tripathi, M. K. and Govil, H., Evaluation of AVIRIS-NG hyperspectral images for mineral identification and mapping. *Heliyon*, 2019, **5**(11), 1–10; doi:10.1016/j.heliyon.2019.e02931.
20. Meer, F. D. V. D. *et al*., Multi- and hyperspectral geologic remote sensing: a review. *Int. J. Appl. Earth Obs. Geoinf*., 2012, **14**(1), 112–128; doi:10.1016/j.jag.2011.08.002.
21. Nouri, T. and Oskouei, M. M., Detection of the geothermal alterations and thermal anomalies by processing of remote sensing data. In XXXIII Asian Conference on Remote Sensing, Sabalan, Iran, 2010.
22. Skinner, B. J., *Introduction to Ore-Forming Processes*, Laurence Robb., Blackwell Publishing, USA, Oxford, Australia, 2005; ISBN 0-632-06378-5.
23. Tripathi, M. K. and Govil, H., Evaluation of analogical analysis techniques in interpretation of lineaments and litho-boundaries using Landsat 7 ETM+ imagery of western Jahajpur. In 4th International Conference on Information Systems and Computer Networks, Calcutta, 2019.
24. Gupta, S. N. *et al*., The precambrian geology of the Aravalli region, southern Rajasthan and north-eastern Gujarat. *Mem. Geol. Surv. India*, 1997, **123**, 262.
25. Sinha-Roy, S., Neotectonically controlled catchment capture: an example from the Banas and Chambal drainage basins, Rajasthan. *Curr. Sci.*, 2001, **80**(2), 293–298.
26. Tripathi, M. K., Govil, H. and Prabhat, D., Lithological mapping using digital image processing techniques on landsat 8 OLI remote sensing data in Jahajpur, Bhilwara, Rajasthan. In 2nd International Conference on Intelligent Communication and Computational Techniques, Manipal University, Jaipur, 28 and 29 September 2019, pp. 43–48.
27. Tripathi, M. K., Govil, H. and Diwan, P., Petrography, XRD analysis and identification of Talc minerals near Chhabadiya village of Jahajpur Region, Bhilwara, India through Hyperion Hyperspectral Remote Sensing Data. In 2nd International Conference on Intelligent Communication and Computational Techniques (ICCT), 2019, pp. 75–78; doi:10.1109/ICCT46177.2019.8969008.
28. Saxena, Asha and Pandit, M. K., Geochemistry of Hindoli Group metasediments, SE Aravalli Craton, NW India: implications for palaeoweathering and provenance. *J. Geol. Soc. India*, 2012, **79**, 267–278; http://mecl.gov.in/Reports/EXE_SUMM_BANERA.pdf
29. Yadav, O. P., Babu, T. B., Shrivastava, P. K., Pande, A. and Gupta, K. R., Short communications and its significance in west Jahajpur basin, Bhilwara district, Rajsthan. *J. Geol. Soc. India*, 2001, **58**, 1–3.
30. Srivastava, R P., Systematic geological mapping in parts of Ajmer, Bhilwara and Udaipur districts, Rajsthan included in topo-sheet nos. 45 K/1&5 (Progress report for the field-season 1966–67), Geological Survey of India, Jaipur, 1968.
31. Heron, A. and Heron, A. M., Synopsis of the pre-Vindhyan geology of Rajputana. *Trans. Nat. Inst. Sci. India*, 1935, **I**, 17–33.
32. Heron, A., The geology of Central Rajputana. In Memoirs of Geological Survey of India, Geological Survey of India, 1953, vol. 79, p. 389.
33. Drusch, M. *et al*., Sentinel-2: ESA's optical high-resolution mission for GMES operational services. *Remote Sensing Environ.*, 2012, **120**, 25–36; doi:10.1080/014311600210092.
34. Abdullah, A., Akhir, J. M. and Abdullah, I., Automatic mapping of lineaments using shaded relief images derived from digital elevation model (DEMs) in the Maran–Sungi Lembing area, Malaysia. *EJGE*, 2010, **15**, 949–957.
35. Adiri, Z. *et al*., Comparison of Landsat-8, ASTER and Sentinel 1 satellite remote sensing data in automatic lineaments extraction: a case study of Sidi Flah-Bouskour inlier, Moroccan Anti-Atlas. *Adv. Space Res.*, 2017, **60**(11), 2355–2367; doi:10.1016/j.asr.2017.09.006.
36. K. M. and Ová, K., Analysis of the relationship of automatically and manually extracted lineaments from DEM and geologically mapped tectonic faults around the main Ethopian rift and the Ehopian highlands. *Ethopia*, 2017, **1**, 5–17.
37. Kocal, A., Duzgun, H. S. and Karpuz, C., An accuracy assessment methodology for the remotely sensed discontinuities: a case study in Andesite Quarry area, Turkey. *Int. J. Remote Sensing*, 2007, **17**, 3915–3936; doi:https:// doi.org/10.1080/01431160601086001.
38. Baidder, L., Khanbari, K., Rhinane, H. and Hilali, A., Using remote sensing for lineament extraction in Al Maghrabah area. In The International Archives of the Photogrammetry, Remote Sensing and Spatial Information Sciences. 3rd International Geoadvances Workshop, Istanbul, Turkey, 16–17 October 2016, vol. XLII-2/w1; doi:10.5194/isprs-archives-XLII-2-W1-137-2016.
39. Tripathi, M. K., Govil, H., Champati Ray, P. K. and Das, I. C., Landslide hazard zonation mapping of Chamoli landslides in remote sensing and GIS environment, 2018; doi:10.5194/isprs-archives-XLII-5-475-2018.
40. Singh, C. P., Science results from Phase-1 airborne hyperspectral campaign with AVIRIS-NG over India, 2017; https://vedas.sac.gov.in/aviris/pdf/AVIRIS_NG_FIRST_PHASE_REPORT.pdf (accessed on 2 June 2018).
41. Ali, S. A. and Ali, U., Litho-structural mapping of sind catchment (Kashmir Basin), NW Himalaya, using remote sensing and GIS techniques. *Int. J. Sci. Res.*, 2015, **4**(7), 1325–1330.
42. Amri, K., Mahdjoub, Y. and Guergour, L., Use of Landsat 7 ETM + for lithological and structural mapping of Wadi Afara Heouine area (Tahifet–Central Hoggar, Algeria). *Arabian J. Geosci*., 2011, **4**, 1273–1287; doi:10.1007/s12517-010-0180-8.
43. Pour, A. B., Hashim, M. and van Genderen, J., Detection of hydrothermal alteration zones in a tropical region using satellite

remote sensing data: Bau goldfield, Sarawak, Malaysia. *Ore Geol. Rev*., 2013, **54**, 181–196; doi:10.1016/j.oregeorev.2013.03.010.
44. Corgne, S., Magagi, R., Yergeau, M. and Sylla, D., An integrated approach to hydro-geological lineament mapping of a semi-arid region of West Africa using Radarsat-1 and GIS. *Remote Sensing Environ.*, 2010, **114**, 1863–1875.
45. Lesage, G., Distribution of district-scale hydrothermal alteration, vein orientations and white mica compositions in the Highland Valley Copper District, British Columbia, Canada: implications for the evolution of porphyry Cu–Mo systems. Thesis, University of British Columbia, 2020; doi:10.1017/CBO9781107415324.004.
46. Rakovan, J., Word to the wise: metasomatism. *Rocks Miner.*, 2005, **80**(1), 63–64; doi:10.3200/rmin.80.1.63-64.
47. Hausrath, E. M., Navarre-Sitchler, A. K., Sak, P. B., Steefel, C. I. and Brantley, S L., Basalt weathering rates on Earth and the duration of liquid water on the plains of Gusev Crater. *Mars Geology*, 2008, **36**(1), 67–70; doi:10.1130/G24238A.1.
48. Greenberger, R. N. *et al*., Imaging spectroscopy of geological samples and outcrops: novel insights from microns to meters. *GSA Today*, 2015, **25**(12), 4–10; doi:10.1130/GSATG252A.1.
49. Tripathi, M. K. and Govil, H., Regolith mapping and geochemistry of hydrothermally altered, weathered and clay minerals, Western Jahajpur Belt, Bhilwara, India. *Geocarto Int*., 2020; https://doi.org/10.1080/10106049.2020.1745302.
50. Govil, H., Tripathi, M. K., Diwan, P., Guha, S. and Monika, Identification of iron oxide minerals in western Jahajpur region, India using avirisng hyperspectral remote sensing. *Int. Arch. Photogramm., Remote Sensing Spat. Infor. Sci. – ISPRS*. 2018, **42**, 233–237; doi:10.5194/isprs-archives-XLII-5-233-2018.
51. Govil, H., Tripathi, M. K., Diwan, P. and Monika, Comparative evaluation of AVIRIS-NG and hyperion hyperspectral image for talc mineral identification. In International Conference on Data Mangement Analytics and Innovation, Turkey, 2019, pp. 95–101.
52. Dey, B., Das, K., Dasgupta, N., Bose, S. and Ghatak, H., Zircon U–Pb SHRIMP dating of the Jahazpur granite and its implications on the stratigraphic status of the Hindoli–Jahazpur Group. In *Seminar Abstract Volume: Developments in Geosciences in the Past Deca*, 2016.
53. Pandit, M. K., Sial, A. N., Malhotra, G., Shekhawat, L. S. and Ferreira, V. P., C-, O-isotope and whole-rock geochemistry of Proterozoic Jahazpur carbonates, NW Indian Craton. *Gondwana Res*., 2003, **6**(3), 513–522.

ACKNOWLEDGEMENT. This work was supported by the Space Applications Centre, Indian Space Research Organisation grant EPSA/4.2/2017 and EPSA/3.1.1/2017.

Received 31 January 2021; revised accepted 14 July 2021

doi: 10.18520/cs/v121/i6/789-800